Correlations between particulate matter emissions and gasoline direct injection spray characteristics

Anbari Attar, Mohammadreza; Xu, Hongming

DOI:
10.1016/j.jaerosci.2016.09.006
10.1016/j.jaerosci.2016.09.006

Document Version
Peer reviewed version

Citation for published version (Harvard):
Anbari Attar, M & Xu, H 2016, 'Correlations between particulate matter emissions and gasoline direct injection spray characteristics', *Journal of Aerosol Science*, vol. 102, pp. 128-141. https://doi.org/10.1016/j.jaerosci.2016.09.006, https://doi.org/10.1016/j.jaerosci.2016.09.006

www.elsevier.com/locate/jaerosci

Correlations between particulate matter emissions and gasoline direct injection spray characteristics

Mohammadreza Anbari Attar, Hongming Xu

PII: S0021-8502(16)30217-8
DOI: http://dx.doi.org/10.1016/j.jaerosci.2016.09.006
Reference: AS5049

To appear in: *Journal of Aerosol Science*

Received date: 25 June 2016
Revised date: 22 September 2016
Accepted date: 23 September 2016

Cite this article as: Mohammadreza Anbari Attar and Hongming Xu, Correlations between particulate matter emissions and gasoline direct injection spray characteristics, *Journal of Aerosol Science* http://dx.doi.org/10.1016/j.jaerosci.2016.09.006

Correlations between particulate matter emissions and gasoline direct injection spray characteristics

Mohammadreza Anbari Attar[a,b*], Hongming Xu[b,c],

[a]Department of Mechanical Engineering, Imperial College London, SW7 2AZ, UK.
[b]Vehicle and Engine Technology Research Centre, University of Birmingham, Birmingham B15 2TT, UK.
[c]State Key Laboratory of Automotive Safety and Energy, Tsinghua University, Beijing, China
[*]Corresponding author at Department of Mechanical Engineering, Imperial College London, SW7 2AZ, UK. Tel: +44 020 7594 2442. E-mail address: m.a.attar@imperial.ac.uk (M. Anbari Attar).

ABSTRACT

The present work investigates impacts of fuel delivery system on Particulate Matter (PM) emissions in a latest generation gasoline Direct Injection Spark Ignition (DISI) engine. Particulate number concentration and size distribution were studied over a wide size range for homogeneous and heterogeneous in-cylinder fuel/air mixtures at different engine speeds/loads. Various fuel spray angles and fuel flow rates were employed to investigate effects of fuel wetting and mixture preparation on particulate emissions. Experimental results highlighted intricate relation between particulate formation/oxidation and engine operating parameters that dictates optimum spray characteristics for lowest PM emissions. The study revealed fuel impingement on hot piston surface during early injection timings and consequent fuel pyrolysis and diffusion flame result in PM size distributions with a peak in accumulation mode (particle diameter ≥50 nm). On the other hand, late fuel impingement on cylinder liner and insufficient time for mixture preparation, result in PM size distributions with a peak around 10-15 nm in nucleation mode. It was concluded that for the latter case, condensation of unburned hydrocarbons was more significant than adsorption into exiting particles' surface.

Keyword: Particulate matter, DISI engine, Spray characteristics, Fuel flow rate

Nomenclature

AED	Aerodynamic equivalent diameter
ATDC	After top dead center
BTDC	Before top dead center
CAD	Crank angle degree
COV	Coefficient of variation
CPC	Condensation particle counter
CS	Catalytic stripper
CVVL	Continuous variable valve lift
DISI	Direct injection spark ignition
DMS	Differential Mobility Spectrometer
ECU	Engine control unit
FIE	Fuel injection equipment
FTP	Federal test procedure
GDI	Gasoline direct injection
MFB	Mass fraction burned
NEDC	New European driving cycle
NMEP	Net mean effective pressure
NSFC	Net specific fuel consumption

PEMS	Portable emissions measurement system
PFI	Port fuel injection
PM	Particulate matter
PMP	Particle measurement program
PN	Particulate matter number
PSD	Particle size distribution
RDE	Real driving emissions
SOI	Start of injection
TD	Thermal denuder
TDC	Top dead center
ULG	Unleaded gasoline
VCT	Variable camshaft timing
VCU	Valve control unit
VPR	Volatile particle remover
WLTC	World harmonized light duty test cycle

1. Introduction

Current powertrain development trends indicate spark ignition engines remain as one of the most dominant power unit types for passenger cars for the coming years. Although, gasoline Port Fuel Injection (PFI) engines are the most common engine type, global production volume of Direct Injection Spark Ignition (DISI) engines will overtake that of the PFI engines. The DISI technologies can improve engine efficiency and performance while reduce gaseous emissions. Albeit, control of Particulate Matter (PM) emissions of the DISI engines is a challenge. Even though DISI engines emit relatively low PM emissions by mass compared to diesel engines, they emit substantial amounts of ultrafine particles. Therefore, Particulate matter Number (PN) concentration and morphology are more relevant metrics than the total PM mass for DISI engines. These particles cover a variety of sizes and are often divided into three size classes: nucleation mode (diameter $(d) \leq 50\ nm$), accumulation mode ($50\ \text{nm} < d < 1\ \mu\text{m}$) and coarse mode ($d \geq 1\ \mu\text{m}$). The chemical compositions of gasoline exhaust PM emissions of PFI and DI engines are well known [1-6]. These particles are generated from four different sources: fuel, lubricant, air and material breakdown. They are composed of different volatile and non-volatile compositions including organic (such as alcohols, aromatics), sulphate (sulphuric acid), nitrate (nitric acid), ash (metals and non-metals) and carbonaceous (mainly soot). Soot as the main component simultaneously form, grow (including: surface grow, coagulation and aggregation) and oxidize during combustion and exhaust process. Soot particles formation from fuel arises from fuel molecules oxidation and pyrolysis which lead to generation of large number of very small ($d < 2$ nm) soot precursors. Carbon/oxygen ratio has been used to define composition of the fuel-oxidizer mixture at onset of soot formation in flames. From equilibrium considerations, soot formation occurs when carbon/oxygen ratio exceeds unity [7]. Hence, in

$$C_m H_n + yO_2 \rightarrow 2_y CO + \frac{n}{2} H_2 + (m - 2y)C \qquad (1)$$

when 'm' becomes larger than '2y'. The corresponding fuel/air equivalence ratio is given by

$$\phi = 2\left(\frac{C}{O}\right)(1 + \delta) \qquad (2)$$

where $\delta = n/(4m)$. Reported in several studies, soot formation typically occurs under locally rich ($\phi > 1.4$) and hot conditions with local temperatures from around 1100 to 1700°C, whereas, soot oxidation is most efficient under stoichiometric to lean conditions, and at temperatures above 1700°C [8-10]. It is believed that the chemistry involved in soot formation has same character in both premixed flame (in spark ignition engines) and diffusion flame (in compression ignition engines). However, soot precursor formation through fuel oxidation and pyrolysis in premixed flames is competing with oxidative attack on these precursors, while in diffusion flames no such attack occurs on precursors [11]. Eventual engine-out soot emission is a balance between the two (soot formation and soot oxidation). Additionally, hydrocarbons in the exhaust gases and atmosphere affect engine-out soot through adsorption into the soot particle surface and condensation to form new particles of hydrocarbon species [12].

Numerous medical studies have linked particulates exposure to health problems. Some researchers subdivide particles based on their Aerodynamic Equivalent Diameter (AED) which defines where they deposit in human body. Three AED fractions of <10, <2.5, and <0.1

μm (PM10, PM2.5, and PM0.1, respectively) are typically used. The World Health Organization estimated that PM2.5 concentration contributes to approximately 800,000 premature deaths per year and ranked it as the 13th leading cause of mortality worldwide [13]. Several studies evaluated PM exposure on cardiovascular [14- 19], respiratory [20-24] and cerebrovascular health effects [25-27]. In addition, some of identified effects of PM on environment include: reduced visibility, increased acidity of lakes and streams, reduced level of nutrients in soil, reduced diversity in ecosystems, damage to stone and other materials [28, 29]. With increasing concern over air quality and human health, regulations for engines' particulate mass were introduced in various countries. However, only the European Commission introduced regulations for DISI engines particulate number [30]. This was initiated as a number of studies on the emission performance of DISI engines showed that while they can easily comply with the PM mass limit, their PN emissions consistently exceed the diesel threshold (e.g. see [31]). Stricter PM legislations in Europe come with change in test cycle from current NEDC (New European Driving Cycle) to new World Harmonized Light Duty Test Cycle (WLTC) which will be used for vehicles certifications. In addition, Real Driving Emissions (RDE) will be implemented into the legislations and Portable Emissions Measurement Systems [PEMS] will be employed. This means particulate emissions have to be studied and reduced over entire engine operation map.

Particulate emissions reduction can be addressed through combustion process or with after-treatment systems. PM emissions reduction potential of Gasoline Particulate Filters (GPF) in after-treatment systems [32- 35] and their development [36- 38] have been investigated in a number of studies. However, due to added complexity and cost of the GPFs (e.g. see [39]), the first approach is still more appealing. Consequently, it is of paramount importance to gain an improved understanding of particulate characteristics and impact of various parameters on their formation and oxidation mechanisms. Some investigators studied PM formation and oxidation mechanism in DISI engines [40- 44] and some focused on reduction techniques via application of new engine hardware or control strategies [e.g. see 45- 49]. Fuel wetting, locally-rich mixture and injector tip coking are considered as the main PM-generating paths in DISI engines. Therefore, the foremost measures for PM emissions reduction in DISI engine are: reducing fuel impingement (on valves, piston and liner), reducing locally-rich areas (via improving mixture preparation and homogeneity) and minimizing injector tip coking. These highlight impacts of fuel delivery system (Fuel Injection Equipment (FIE) and control strategy) on PM emissions in DISI engines.

A survey of available publications on internal combustion engines' PM emissions indicates smaller number of reports on DISI engines compared to compression ignition engines. Adding to this, nature of DISI engine particulate emissions (more volatile and smaller particles, which are difficult to measure) and complexity of these systems when compared to diesel engines make comparison of the available PM emissions data a perplexing task. Recent evolution of gasoline Fuel Injection Equipment (FIE), valvetrain and ignition systems, employment of alternative combustion strategies (e.g. homogeneous charge compression ignition or gasoline compression ignition) and fuel blends have spread the available experimental data and introduced some discrepancies. Consequently, there is a demand for further experimental data. The present work is an investigation into effects of purpose-designed FIE, operating parameters and control strategies on PM emissions to attain a better undressing of PM generating paths in order to identify routes for further PM emissions reduction in advanced DISI engines.

2. Experimental setup and methodology

2.1. Test engine

Table 1 summarizes specifications of the test engine; a single cylinder spray-guided DISI engine with a pent-roof combustion chamber and a centrally mounted injector. Engine head exploited a Variable Camshaft Timing (VCT) system with 50 CAD camshaft phasing on exhaust and intake sides, a Continues Variable Valve Lift (CVVL) system (with 1 to 10 mm valve lift adjustment) on the intake side. An open Engine Control Unit (ECU) was used to adjust camshafts phasing, air-fuel ratio, injection and spark timing. A separate Valve Control Unit (VCU) was used to adjust intake valves' lift. Both the ECU and the VCU were controlled via INCA software. Solenoid-actuated multi-hole injectors were used with a cam-driven fuel pump at 200 bar fuel pressure. Engine was coupled to a Sierra-CP 70 kW AC dynamometer and controlled via CADET control and data acquisition system. During the tests, engine oil (5W20) and coolant temperature were controlled at 50°C with an accuracy of ±1°C. In order to reduce systematic errors and due to length of experimental tests, all temperature and pressure sensors were calibrated periodically using Beamex MC4 calibrator. Market fuel (unleaded gasoline, ULG95) was used in all tests. Water-cooled Kistler piezoelectric pressure transducer was used to acquire in-cylinder pressure data. Batches of 300 consecutive pressure cycles were acquired via AVL Indicom acquisition system to evaluate combustion performance. Although engine crank angle encoder (AVL 365C) could have output pulses of 0.025 CAD, the Indicom acquisition system resolution was limited to 0.1 CAD. For each test, start of Injection (SOI) was swept over an extended window and injection pulse width was adjusted to achieve the required load at lambda 1; spark timing was adjusted for 50% Mass Fraction Burned (MFB 50%) at 8 CAD ATDC over the SOI sweep window. Schematic diagram of the experimental setup is presented in Figure 1. Table 2 summarizes the operating conditions.

Table 1 Key engine specifications

Combustion chamber design	Pent-roof with a centrally mounted injector
Displaced volume	450 cc
Bore × stroke	83 mm × 92 mm
Compression ratio	10:1
Intake/Exhaust valve diameter ratio	1.14
Valve lift	Intake: 1 to10 mm, Exhaust: 10 mm fixed
Camshaft phasing	Intake: 50 CAD, Exhaust: 50 CAD
Injector type	Solenoid-actuated multi-hole (laser drilled)

Table 2 Engine operating conditions

Test	Impacts of FIE
Engine speed (rpm)	1500, 2000
Engine load (NMEP bar)	5, 8
Coolant/oil temperature (°C)	50 ±1
Start of injection (CAD BTDC)	330 to 250 with 10 CAD intervals
Spark timing	Adjusted for MFB 50% at 8 CAD ATDC
Fuel rail pressure (bar)	200 ± 0.1
Fuel	ULG95
Lambda	1
Camshaft phasing (CAD)	Intake: 25, Exhaust: 25
Intake valve lift & throttle position	Max lift with variable throttle position

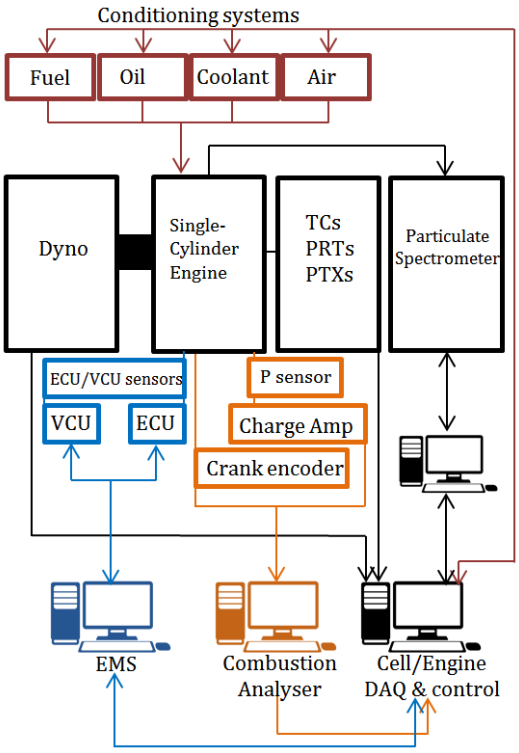

Fig. 1. Schematic diagram of the experimental setup

2.2. Fuel injection system; fuel spray angle and fuel flow rate

A number of studies have investigated effects of fuel injection pressure on PM emissions reduction from DISI engines [e.g. see 50]. Elevated injection pressures can reduce PM emissions by reducing injector tip deposit formation [51]. This deposit can build up inside injector nozzles, alter spray pattern and increase charge stratification that leads to a higher number of locally rich regions [52]. Also deposit can form on injector tip surface, absorb fuel and eventually burn in pool fire [53, 54]. In addition, higher fuel rail pressures can enhance spray atomization and fuel-air mixing which reduce fuel penetration length and fuel wetting. In general, spray-guided DISI engines have less fuel impingement on piston crown compared with wall-guided DISI engines. Nevertheless, fuel impingement on valves, liner and piston crown is one of the main contributors to the PM emissions from spray-guided DISI engines. On the injector side, fuel plumes targeting and penetration length are key parameters in controlling fuel wetting. Plumes penetration length itself depends on fuel break up. Fuel breakup and atomization relies on turbulence energy of injected fuel and shearing force between fuel and air [55]. The shearing force itself is proportional to liquid fuel velocity. Both the turbulence energy and velocity of the injected fuel are governed by Bernoulli's relation, which states a trade-off between their magnitudes. Thus the fuel penetration length (from injector nozzle to point of spray breakup) can be expressed by:

$$l_b = 2a(1.03We^{0.5})ln\left(\frac{a}{\beta_0}\right) \quad (3)$$

$$W_e = p_l U^2 \left(\frac{a}{\sigma_t}\right) \quad (4)$$

Where a is diameter of the injected fuel flow, β_0 is the fluctuation wave vibration amplitude caused by turbulence energy, U is fuel velocity, p_l is fuel density, σ_t is fuel surface tension [55]. For better fuel atomization and reduced spray penetration, fuel velocity should be reduced and the fluctuation wave needs to be increased. Converting fuel pressure energy into turbulence energy rather than velocity can be achieved by optimizing injector nozzle geometry and its fine positioning [56]. Therefore, no significant improvement in fuel

atomization should be expected by solely increasing fuel pump pressure without an appropriate and compatible nozzle design [e.g. see 57]. As the higher injection pressure can increase system costs and pumping work, some studies focused on nozzle hole design and advanced manufacturing techniques [e.g. see 50] in order to meet the PM emissions regulations at today's 200 bar pumps operating pressure. In this work, nozzle hole design; spray angle and fuel flow rate were investigated to explore effective and cost competitive solutions. Six laser-drilled injectors were studied in this work. Each utilized six nozzle holes with pre chambers arranged in a circular pattern. Required fuel flow rate was determined by the number of injector holes and holes' diameter. The pre chamber geometry was determined by combination of spray pattern and coking performance testing. Individual plume targeting was carried out through CFD investigation in order to achieve an optimized spray pattern that matches the specific combustion chamber layout. Effects of three spray patterns (B2, B1 and J1, shown in Figure 2) and two fuel flow rates for each pattern were investigated. The B2 injectors had the widest spray angle and the J1 injectors had the narrowest spray angle. The B1 injectors' spray angle was between the B2s' and J1s'. The nominal fuel flow rate of the high-flow (H) injectors was 15% higher than the low-flow (L) injectors.

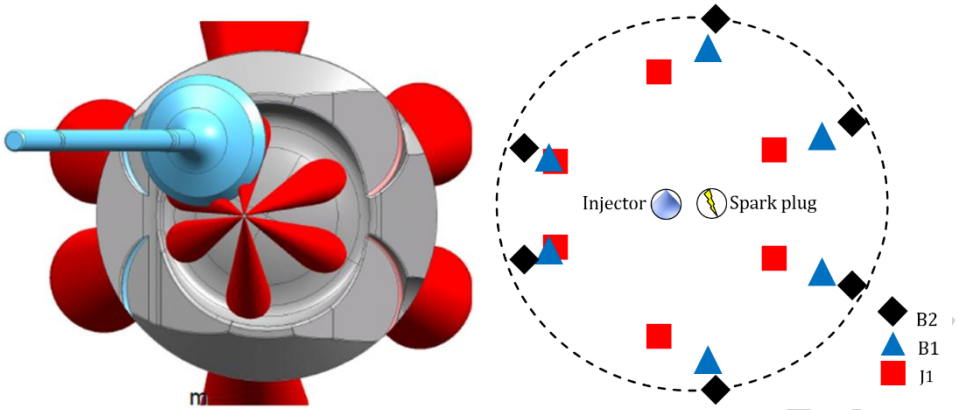

Fig. 2. Left: CFD plume targeting of the B1 injectors, Right: overlaid plumes' footprint.

2.3. Particulate matter measurement

Particulate number concentration and size distribution were measured using Cambustion DMS500 Fast Particulate Spectrometer. The device is a non-certification system. Regulation-compliant PM measurement systems that comply with the UN/ECE Particle Measurement Program (PMP) have a Volatile Particle Remover (VPR) to eliminate liquid particles, and a Condensation Particle Counter (CPC) to count solid particles that remain. The DMS500 system utilizes a different measurement technique. It combines electrical mobility measurements of particles with sensitive electrometer detectors, to give outputs of particle size, number and mass in real time [58, 59]. The device has ~5% uncertainty in particle size measurement for particles smaller than 300 nm and ~10% uncertainty for larger particles. For the particle number, measurement uncertainty is ~10% over the full spectrum. A recent comparison of a number of commercially available systems under steady-state conditions indicated a good correlation between readings from DMS500 system and regulation-compliant systems including Horiba SPCS Particle Counter, and AVL Particle Counter (APC) [43, 60]. In addition to the measurement technique, PM emissions level is sensitive to sampling methodology [61, 62]. Johansson et al. [63] compared DMS500 sampling system with a commercially available particle sampler, Dekati FPS-4000 with thermal denuder (TD), in order to investigate contribution of volatile particles. They reported while both sampling systems show similar PM size distribution, the DMS500 sampling system detected more particles especially below 20 nm with reduced measurements' stability. Swanson et al. [62] compared thermal denuder (TD) and catalytic stripper (CS) methods. While in the TD method, semi-volatile materials are removed by adsorption, in the CS method, heated and diluted exhaust pass over a heated oxidation catalyst. They proposed the CS method as the superior method due to incomplete removal of evaporated compounds in the TD method which introduced measurements artifacts. However, it should be noted that the evaporation of the volatile particles in these techniques inevitably affects solid particles as well. In addition, when exhaust temperature falls, volatile components are transferred into solid phase, adhering to existing particles or nucleating into new particles [64]. In the present work, DMS500 was connected directly to engine exhaust flow via its heated sampling line close to the exhaust port. The DMS500 engine sampling system incorporates two stages of dilution. The first diluter uses compressed dry air metered by the DMS500 for low ratio dilution up to 5:1. This diluter is placed at the head of the heated sample line which was connected directly to the engine exhaust port. Sample flow rate was 7.6 l/m and the heated line temperature was set at 150°C to avoid nucleation of hydrocarbons. The second diluter uses a rotating disc to provide high dilution ratios which can be varied to maintain good signal to noise ratio. This dilution ratio was adjusted automatically between 1:1 and 20:1. Although the current lower cut-off size of the PMP methodology is 23 nm, in this work, particles were measured from 5 nm to 1000 nm. Some investigators have examined number emissions of solid particles below 23 nm [2, 65, 66]. Khalek et al. [5] concluded that 15 to 20% of total emitted solid particles from a stoichiometric GDI vehicle (over Federal Test Procedure (FTP) and US06 test cycles) are smaller than 23 nm.

The test engine was a latest technology DISI engine designed to meet the current gaseous and particulate emissions legislations. Under steady-state and fully warmed-up conditions over majority of test points, PN concentration was close to instrument noise base level (~390 #/cc). The low PN concentration level reduced instrument signal to noise ratio and raised questions on data plausibility on these points. Therefore, all tests in this work were carried out with both engine coolant and lubricating oil temperature set at 50°C. It should be noted that the total PN concentration noise base level of the instrument was calculated by adding up all size class data for the noise (measured during instrument auto-zero process prior to measurement; shown in Figure 3), multiplying the sum by instrument dilution factor and dividing the total by the number of size classes. To attain satisfactory data for comparative study, all measurements were carried in an identical manner with engine conditioning process and combustion parameters under strict control. Injectors were cleaned

in ultra-sonic bath prior to each SOI sweep test. Combustion stability was always better than 1.2% COV of NMEP, typically between 0.4% and 0.9%. The instrument sampling frequency was 10 Hz. However, in order to improve measurement signal to noise ratio, data obtained at 10 Hz was averaged over 10 samples; thus output data frequency was reduced to 1 Hz. All measurements were carried out under steady-state condition for 120 s and time-averaged using the manufacturer software. At the end of each SOI sweep test; PM measurements at two SOI points were repeated. One point was the repeat of the first SOI point and the other was chosen randomly from test matrix. The repeats were used to investigate any drift in measurements and that the measurements were carried out with acceptable repeatability.

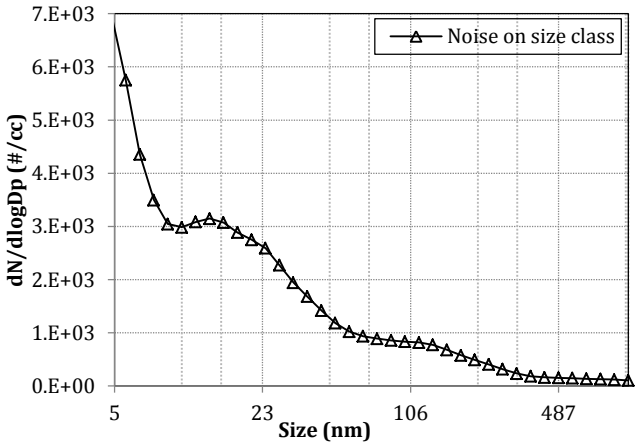

Fig. 3. Instrument noise on each particulate size class

2.4. Engine PM emissions baseline

In order to obtain engine-out PM emissions baseline and determine contribution of engine oil and material breakdown, engine was adapted to run on methane through the use of a PFI rail. Tests were carried out at 2000 rpm at 5 bar and 8 bar NMEP with lambda set at 1.15. PM emissions measurements were carried out at steady sate condition. Injection timing was set at 330 CAD BTDC. Ignition timing was set for 50% MFB at 8 CAD ATDC. Figure 4 shows PM size distribution at both loads. In general, the PM emissions at both loads were very low. A crosscheck with Figure 3 (instrument noise level on each size class) indicated that the data is very close to the noise level. As the test engine was a new engine, we did not expect any significant contribution from martial break down (e.g. wearing piston rings) or deposit breaking off from combustion chamber surface. Therefore the PM emissions were associated with the engine lubricating oil and the hydrocarbon fuel. (Deleted section)

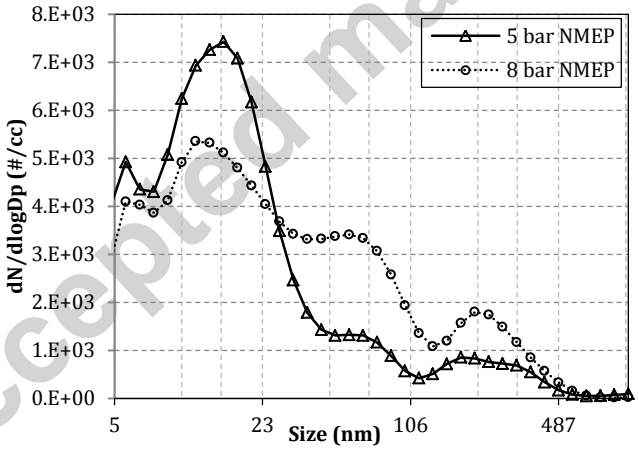

Fig. 4. Number-weighted particle size distribution for engine running on methane at 2000 rpm/5 bar and 8 bar NMEP

3. Results and discussion

Although retarded (late) injection timings during compression stroke can benefit from higher in-cylinder charge temperature for fuel vaporization, they are avoided due to lack of adequate in-cylinder charge motion and insufficient time for mixture preparation [e.g. see 67]. Advanced (early) injection timings are also avoided due to piston wetting [67, 68]. Therefore, a very limited time during intake and compression strokes is available for fuel injection at different engine operating conditions. In the present work, in order to have a better understanding of fuel impingement and mixture preparation effects on PM emissions, a relatively wide SOI sweep window was investigated. Injection timings from 330 to 250 CAD BTDC were studied. We divided this extended SOI sweep window into 'early' SOIs from 330 to 300 CAD BTDC and 'late' SOIs from 290 to 250 CAD BTDC. Figure 5 (a) shows total particulate number concentration of all six injectors for the late SOIs. It was observed that over the SOI sweep from 290 to 250 CAD BTDC, the total PN increased for the B1 and the B2 injectors with wider spray angles while the total PN reduced for the J1 injectors with a narrowest spray angle. Due to piston position at these injection timings and spray angle, we did not expect any piston wetting from the B1 and the B2 injectors. Hence, main contributors to the total PN concentration were considered to be: poor mixture preparation and cylinder liner wetting. Higher total PN values for the B2 injectors compared to the B1 injectors, were associated with the liner wetting; the B1 narrower spray angle provided a

longer path for injected fuel to travel before it hits the liner. For the J1 injectors, the total PN increased as injection timing was advanced, indicating contribution of piston wetting even at these late injection timings. For these SOIs, higher fuel flow rate resulted in lower total PN. This was due to a higher spray momentum for the high-flow injectors that enhanced fuel atomization and provided a better mixture. Furthermore, the enhanced fuel atomization also reduced plumes' penetration length and liner wetting. Figure 5 (b) shows total PN concentration for the early SOIs. For these SOIs, wider spray angles resulted in lower total PN, while higher fuel flow rate increased total PN. At these early injection timings, piston was very close to the injector tip. This promoted piston wetting and pool fire which significantly increased PM emissions. With the wide spray angles, injected fuel could travel a longer distance before hitting the piston surface. Both the available penetration length and time improved fuel evaporation and reduced fuel impingement. Highest PN levels were observed for the J1 injectors with the narrowest spray angle and lowest PN levels for the B2 injectors with the widest spray angle. For the high-flow injectors, injection pulse width (injection duration) was reduced to maintain same engine load. Considering that the piston was moving downward, shorter injection duration resulted in more fuel impingement when the piston was close to the injector tip. Consequently, for the early SOIs, higher fuel flow rate increased the total PN. This effect was less significant for the wider spray angles due to longer plumes' penetration length.

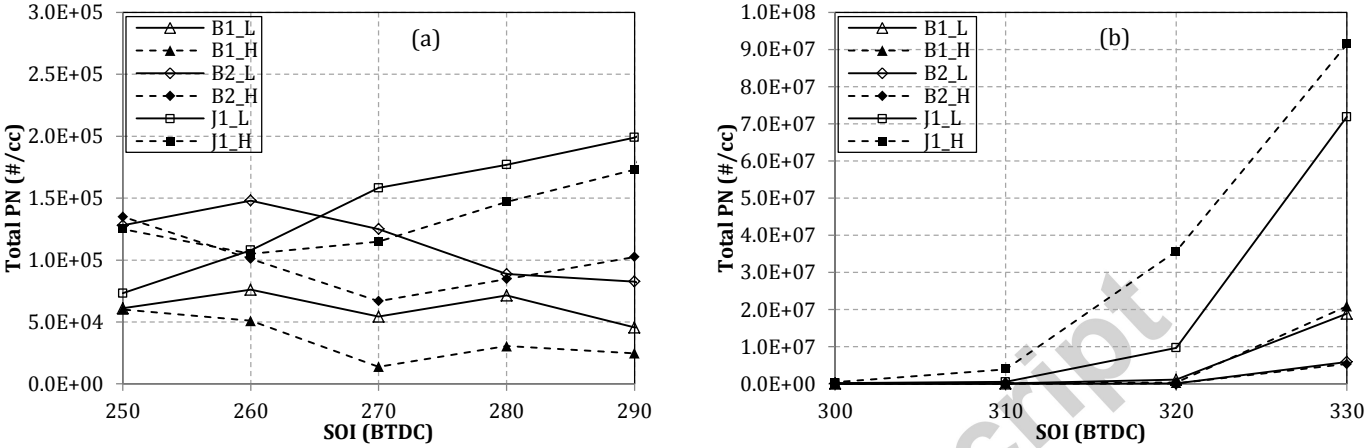

Fig. 5. Total PN concentration at 1500 rpm/5 bar NMEP for: (a) late SOIs, (b) early SOIs

Figure 6 shows number-weighted Particle Size Distribution (PSD) for each injector averaged over the SOI sweep window. The PSDs for the J1 injectors are plotted on secondary axis. All injectors showed similar particle size distribution with a peak in the accumulation mode. It was observed that injectors' flow rate has no significant effect on the PSDs, while spray angle altered the PSDs. Wider spray angles shifted peak of the size distributions towards smaller particles; so, the peak of the PSD for J1, B1 and B2 injectors occurred at 133 nm, 115 nm and 100 nm, respectively. Although this figure provided an overall view of impact of each injector on particle size distribution, as these PSDs are averaged over the entire SOI sweep window, they are skewed towards injection timings with highest PN concentration.

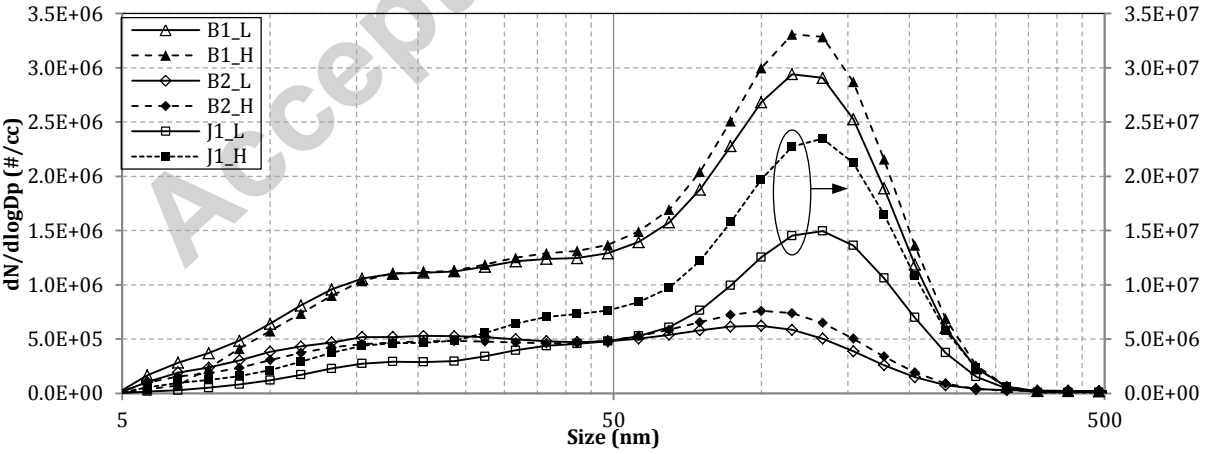

Fig. 6. Number-weighted particle size distribution averaged over SOI sweep window, 1500 rpm/5 bar NMEP

Therefore, out of six tested injectors, two opposite cases were chosen in order to further probe impacts of spray angle and fuel flow rate on particle size distribution. These two injectors were J1_H injector (with the narrowest spray angle and high flow rate) and B2_L (with the widest spray angle and low flow rate). As it was discussed earlier, the J1_H injector had the most severe piston wetting during the early SOIs. Figure 7 and Figure 8 present PSD for each injection timing for the J1_H injector. All injection timings showed bimodal PSD with a peak in the accumulation mode and a peak in the nucleation mode. For the early SOIs, as the injection timing was retarded, PN

concentration reduction was more dominant in the accumulation mode than the nucleation mode. This was associated with mechanisms involved in particulate precursor formation and will be discussed later in this section. For SOIs between 330 and 300 CAD BTDC accumulation mode peak was reduced from 1.66×10^{8} to 3.79×10^{5} #/cc. For SOI at 310 CAD BTDC at which piston wetting effect was picked up, the primary and the secondary peaks had almost same amplitude. Also, while for all SOIs the primary peak occurred between 100 and 115 nm and the secondary peak around 11-13 nm, for the SOI at 310 CAD BTD, these peaks shifted towards each other to 65 and 18 nm for the secondary and the primary peak, respectively. This shift in PSD for the SOI at 310 CAD BTD will be discussed later in this section. For the late SOIs between 290 and 250 CAD BTDC, as the injection timing was retarded, number of emitted particles below ~31 nm increased while number of particles emitted above ~31 nm decreased. Figure 9 presents PSD for each SOI for the B2_L injector. Particle size distribution of the SOI at 330 CAD BTDC is plotted on a secondary axis. PSDs for the early SOIs were bimodal. The PSD of the earliest injection timing at 330 CAD BTDC was similar to PSDs during the early SOIs with the J1_H injector. This was in agreement with Figure 5 (b) where piston wetting effect significantly increased PN concentration at this SOI for the B2_L injector. As the injection timing was retarded, the PN concentration level dropped to the lowest for the optimum injection timings at 300 and 290 CAD BTDC. As the injection timing was further retarded and for the latest three SOIs (280, 270 and 260 CAD BTDC), due to poor mixture preparation, the PN concentration level increased again and the particle size distributions became unimodal with a peak in the nucleation mode. Crosscheck of Figure 8 and Figure 9 suggested that advanced injection timings and fuel impingement on piston promoted accumulation mode particles while late injection timings and liner wetting, in-cylinder charge stratification and poor mixture preparation promoted nucleation mode particles.

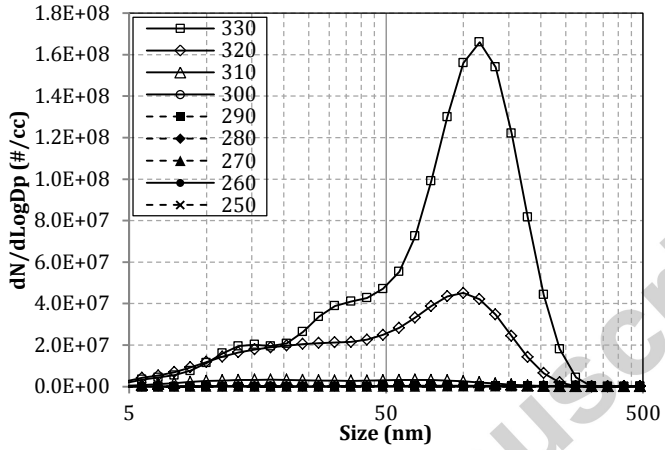

Fig. 7. Number-weighted particle size distribution for individual SOIs, J1_H injector, 1500 rpm/5 bar NMEP

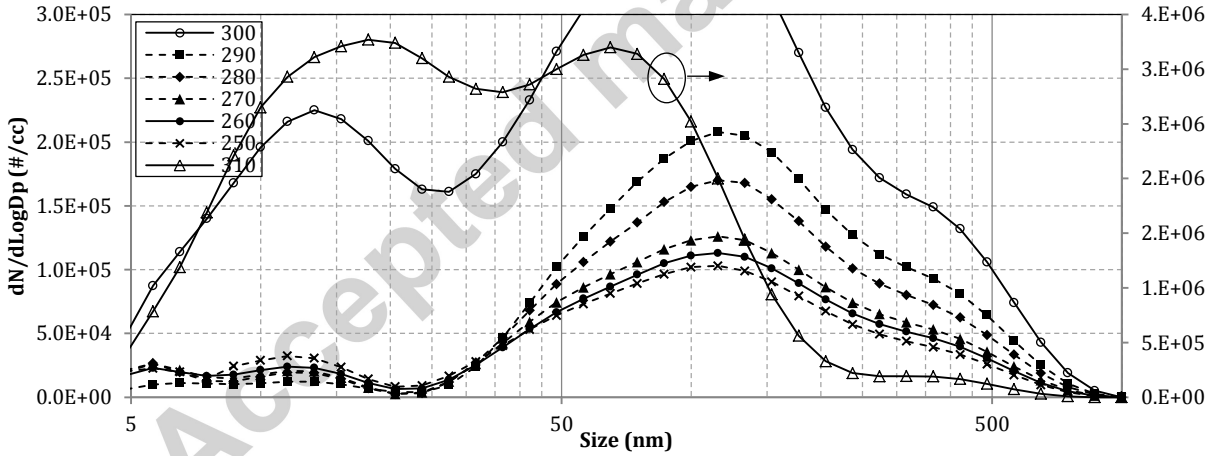

Fig. 8. Number-weighted particle size distribution for each SOI, J1_H injector, 1500 rpm/5 bar NMEP

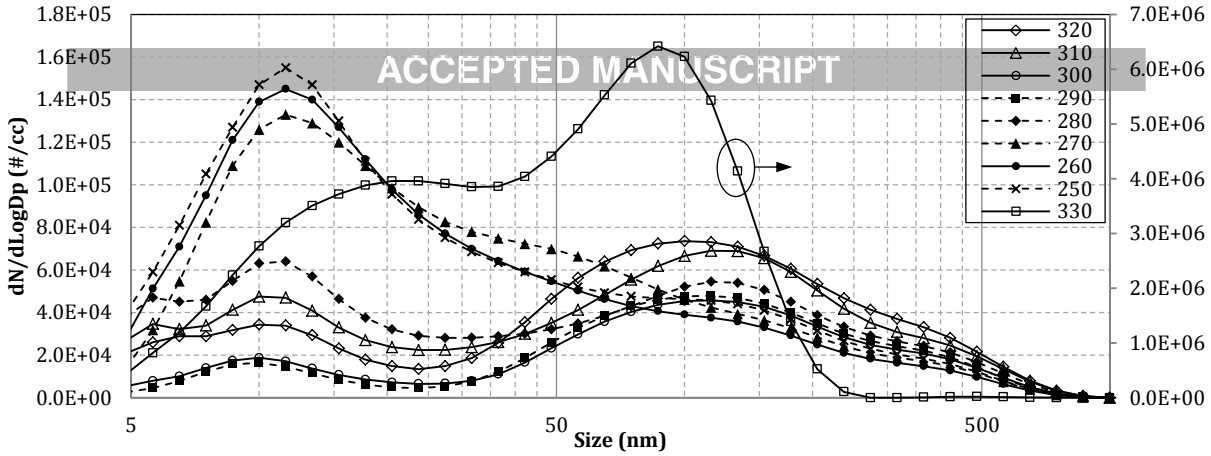

Fig. 9. Number-weighted particle size distribution for each SOI, B2_L injector, 1500 rpm/5 bar NMEP

In order to examine impacts of engine speed and load on PM emissions, tests were repeated at 2000 rpm/8 bar NMEP and results were compared with data obtained at 1500 rpm/5 bar NMEP. Figure 10 (a) and (b) present results for the late and the early SOIs, respectively. For the early SOIs, similar trends to the lower speed/load tests (Figure 5, b) were observed. Widest spray angle and higher fuel flow rate produced higher total PN, albeit, at significantly lower levels. Also, while at 1500 rpm/5 bar NMEP, the piston wetting effect was picked up for SOI at 310 and 320 CAD BTDC for the J1_H and the J1_L injectors, respectively, at 2000 rpm/8 bar NMEP, these were shifted by 10 CAD for both injectors. The lower total PN and the shifted PN pickup points were associated with higher in-cylinder charge temperature and higher piston surface temperature at the higher engine speed/load that promoted fuel vaporization. For the late SOIs, in general, higher total PN concentration was measured at 2000 rpm/8 bar NMEP compared to 1500 rpm/5 bar NMEP. However, some similar trends to the lower speed/load results were observed. Higher fuel flow rate resulted in lower total PN, suggesting advantage of high-flow injectors in mixture preparation. Also the total PN concentration of both B1 and B2 injectors was increased by retarding injection timing. This trend was more significant at the higher speed/load compared to the lower speed/load. This was associated with both higher injected fuel quantity at higher engine load and shorter available time for fuel evaporation and mixture preparation at higher engine speed. As in lower speed/load case, the B2 injectors showed higher total PN concentration compared to the B1 injectors. This was linked with more severe cylinder liner wetting at late SOIs.

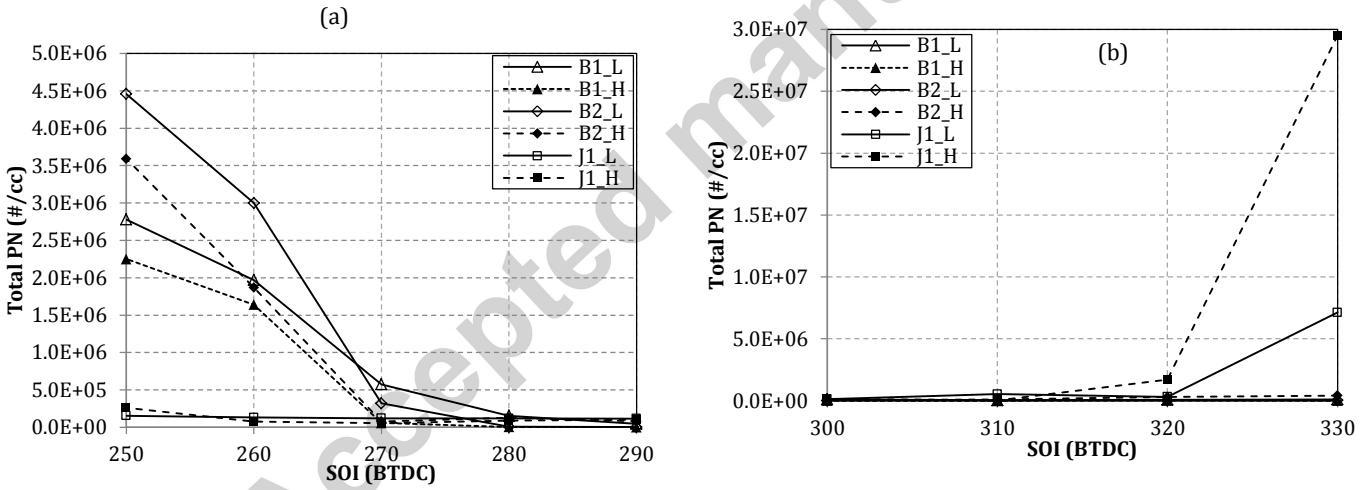

Fig. 10. Total PN concentration 2000 rpm/8 bar NMEP for: (a) late SOIs, (b) early SOIs

Figure 11 presents number-weighted particle size distribution averaged over the SOI sweep window at 2000 rpm and 8 bar NMEP for all six injectors. The PSD from the J1_H injector is plotted on a secondary axis. In general, the averaged PSDs were shifted towards smaller particles at the higher speed/load. Impact of spray angle on PSDs was clearer at this higher speed/load. The J1_H (narrowest spray angle) and the B2_L (widest spray angle) injectors showed unimodal particle size distributions that mirrored each other. The J1_H PSD was skewed towards the accumulation mode particles with a peak at 100 nm. The B2_L PSD was skewed towards the nucleation mode particles with a peak at 15 nm. The B1 injectors showed bimodal particle size distributions and displayed transition between PSD of the J1_H and PSD of the B2_L. Impact of fuel flow rate was distinct at the higher speed/load. For the J1 injectors which suffered from piston wetting, lower fuel flow rate reduced number of accumulation mode particles by about five folds (at 100 nm) while number of nucleation mode particles reduced by less than three folds (at 15 nm). For the B2 injectors which suffered from poor mixture preparation and more severe liner wetting, the higher fuel flow rate, reduced number of nucleation mode particles while increased number of accumulation mode particles.

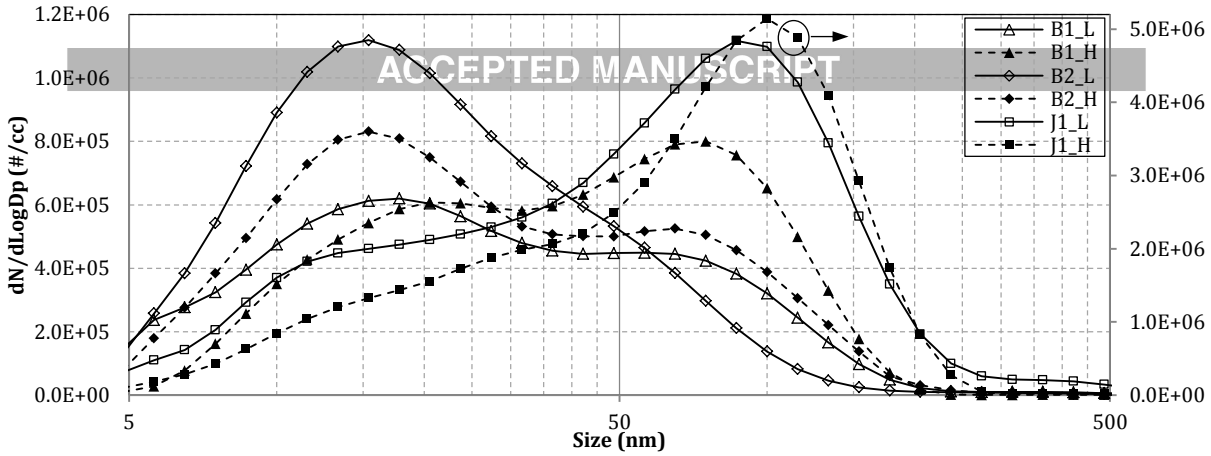

Fig. 11. Number-weighted particle size distribution averaged over SOI sweep window, 2000 rpm/8 bar NMEP

Similar to the previous section, out of six injectors, two injectors with distinct opposite PSDs were selected to further investigate impacts of spray angle and fuel flow rate on particle size distribution at the higher engine speed/load. Figure 12 and Figure 13 present number-weighted particle size distribution for each injection timing over the SOI sweep window for the J1_H and the B2_L injectors, respectively. For the J1_H injector, except for the earliest injection timing that showed unimodal PSD with a peak in the accumulation mode, all other injection timings had bimodal PSD. As the injection timing was retarded number of accumulation mode particles reduced while number of nucleation mode particles increased. For the B2_L injector, except for the earliest injection timing, all other injection timings had unimodal PSD with a peak in the nucleation mode. As the injection timing was retarded, the nucleation mode peak amplitude increased. For the earliest injection timing at 330 CAD BTDC, we could still observe effects of piston wetting on PSD and the primary peak in the accumulation mode particles. As it is shown in Figure 13, for the B2_L injector with late SOIs, the primary peak was located around 13 to 17 nm which was below the current 23 nm lower cut-off size of the PMP methodology; indicating how emissions standards can affect engine calibration and the choice between engine hardware.

Comparison of particle size distribution for these purposed-designed injectors at both speeds/loads indicated that while fuel impingement always increased number of emitted particles, its effects on particle size distribution was determined by location of fuel wetting and its relative timing. It was observed that early piston wetting significantly increased number of accumulation mode particles while late liner wetting mainly increased number of nucleation mode particles. When fuel hits a cold piston surface, it form a liquid film. This fuel film does not burn during primary combustion but it burns in diffusion flame after end of the primary combustion. Both high temperature and locally fuel-rich areas promote generation of particulate precursors in diffusion flame. Surface growth, coagulation and aggregation increase diameter of these precursors. These three mechanisms result in number-weighted particle size distribution with a peak in the accumulation mode, if there is enough time for particles' growth. As it was observed in Figure 7 and Figure 8, by retarding the SOI from 330 to 310 CAD BTDC, PN concentration dropped (as the fuel impingement was reduced) and at the same time, the accumulation mode peak of the PSDs was shifted towards smaller particles (as there was less available time for particles' growth). In this test, the accumulation mode peak was occurred at 115, 100 and 65 nm for SOI at 330, 320 and 310 CAD BTDC, respectively. When piston temperature is high, it can vaporize part of impinged fuel. Advanced injection timing provides sufficient time for the vaporized fuel to mix with in-cylinder charge and produce a homogeneous mixture. Therefore, engine can even benefit from piston wetting if piston surface temperature and amount of impinged fuel lead to a better mixture preparation. However, when fuel quantity is high, it forms a liquid fuel film on the piston which burns in diffusion flame same as in the cold piston case. In addition, with high piston surface temperature, fuel pyrolysis can occur which is another source of particulate formation. Hydrocarbon thermal cracking, dehydrogenation, condensation and polymerization are considered as main pyrolysis mechanisms that depend on hydrocarbon species and temperature [69, 70]. Condensation and polymerization create larger molecules. Thermal cracking results in fragmentation of fuel molecules into smaller ones. Dehydrogenation lowers hydrogen to carbon ratio of the hydrocarbons to become soot. All these mechanisms ultimately produce particulate precursors that can further grow during and after combustion. On the other hand, when fuel hits cylinder liner it is mainly absorb by a thin oil layer on the liner. The absorbed hydrocarbon components escape primary combustion process unburned and are desorbed after the end of combustion. These gas-phase species contribute to engine-out PM emissions by either condensation where they form new particles or adsorption into exiting particles' surface and incorporation into particulate phase. The latter increases particulate mass emission but has no impact on particulate number. Therefore, high PN concentration observed for the late SOIs indicated that the main mechanism was condensation of unburned hydrocarbons. As these particle precursors form after the primary combustion at lower temperatures and pressures they cannot grow as much as the precursors that form during the primary combustion. Consequently, their size distribution are skewed towards the nucleation mode.

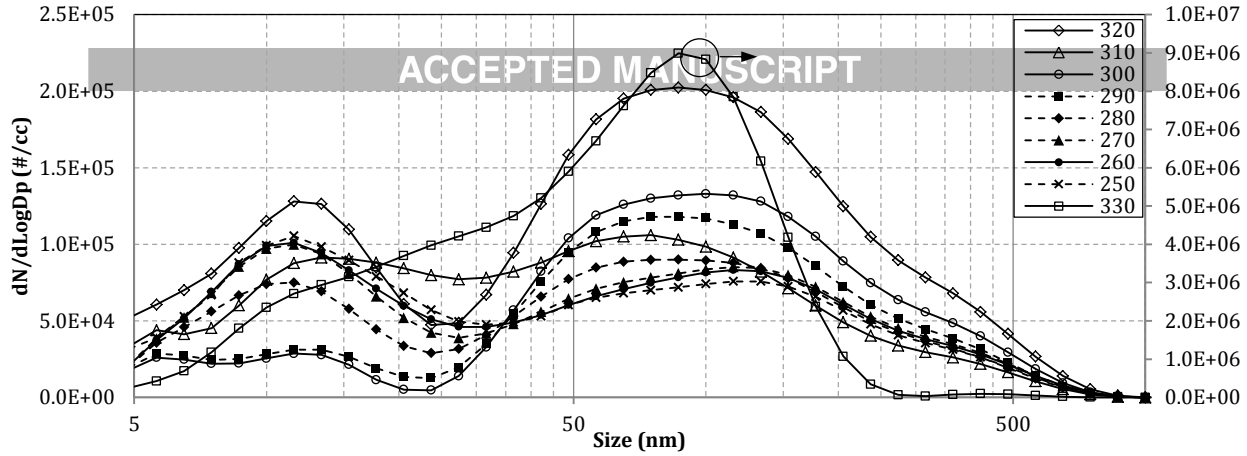

Fig. 12. Number-weighted particle size distribution for each SOI, J1_H injector, 2000 rpm/8 bar NMEP

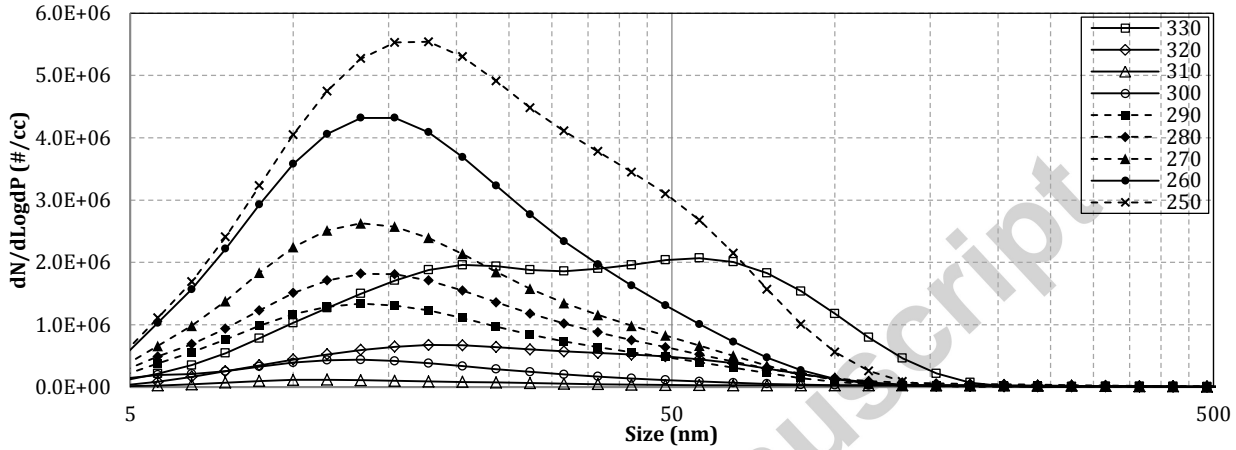

Fig. 13. Number-weighted particle size distribution for each SOI, B2_L injector, 2000 rpm/8 bar NMEP

4. Conclusions

Experimental measurements of engine-out particulate emissions were conducted on a latest technology single cylinder spray-guided DISI engine. Six different injectors (three spray angles, each with two fuel flow rates) were tested at two engine speeds/loads. Due to significantly low PM emissions with the fully warmed-up engine, tests were carried out at 50°C engine coolant and lubricating oil temperature. Based on the results, following conclusions have been made:

- For early injection timings, wider spray angles and lower fuel flow rate decreased total PN concentration. The main contributor to PM emissions was fuel impingement on the piston surface. Wider spray angles extended available penetration length and time for fuel evaporation before the plumes hit the piston surface. The lower fuel flow rate, extended injection duration and reduced fuel injection quantity when the piston was close to the injector tip.
- For late injection timings, contradictory to the early injection timings, wider spray angles and lower fuel flow rate increased total PN concentration. The main contributors to the PM emissions were poor mixture preparation and liner wetting for the wide spray angles. The higher fuel flow rate was beneficial in PM emissions reduction as it provided higher spray momentum which enhanced mixture preparation and reduced plumes' penetration length.
- At the higher engine speed/load, for the early injection timings, total PN concentration was significantly reduced for all injectors and no significant piston wetting effect was observed for the wide spray angles. This was associated with higher in-cylinder charge temperature and higher piston surface temperature which enhanced fuel vaporization prior to ignition. Impacts of spray angle and fuel flow rate on PM emissions for the narrowest spray angle were similar to the tests at the lower engine speed/load.
- At the higher engine speed/load, for the late injection timings, total PN concentration was higher compared to the lower speed/load. This was associated with higher injected fuel quantity at the higher engine load and shorter available time for mixture preparation at the higher engine speed. Impacts of fuel flow rate and spray angle were similar to the tests at the lower speed/load.
- Investigation of number-weighted particle size distribution revealed that fuel impingement on piston surface during early injection timings promoted accumulation mode particles. This was associated with available time provided by the early injection timings and high in-cylinder pressures and temperatures during primary combustion that allowed further growth of particle precursors that formed via fuel pyrolysis and in diffusion flame. On the other hand, it was concluded that fuel impingement on cylinder liner and poor mixture preparation from late injection timings promoted nucleation mode particles via condensation of unburned hydrocarbon.

Acknowledgements

This work was conducted in Future Engines and Fuels Laboratory at University of Birmingham. The authors gratefully acknowledge technical and financial support of the laboratory by Jaguar Land Rover plc and Shell Global Solutions (UK). Great thanks are extended to Rickie Creegan and Lucas Miles Polglase for their help running engine tests.

References

1. Andersson, J., Wedekind, B., Hall, D., Stradling, R. et al., "DETR/SMMT/CONCAWE Particulate Research Programme: Light Duty Results," SAE Technical Paper 2001-01-3577, 2001, doi:10.4271/2001-01-3577.
2. Mohr, M., Lehmann, U., and Margaria, G., "ACEA Programme on the Emissions of Fine Particulates from Passenger Cars(2) Part1: Particle Characterisation of a Wide Range of Engine Technologies," SAE Technical Paper 2003-01-1889, 2003, doi:10.4271/2003-01-1889.
3. Bosteels, D., May, J., Karlsson, H., and de Serves, C., "'Regulated' and 'Non-regulated' Emissions from Modern European Passenger Cars," SAE Technical Paper 2006-01-1516, 2006, doi:10.4271/2006-01-1516.
4. Schauer J.J., Christensen C. G., Kittelson D. B., Johnson J.P. and Watts W. F. (2008). "Impact of Ambient Temperatures and Driving Conditions on the Chemical Composition of Particulate Matter Emissions from Non-Smoking Gasoline-Powered Motor Vehicles," Aerosol Science and Technology, 42:3, 210-223, DOI: 10.1080/02786820801958742.
5. Khalek, I., Bougher, T., and Jetter, J., "Particle Emissions from a 2009 Gasoline Direct Injection Engine Using Different Commercially Available Fuels," SAE Int. J. Fuels Lubr. 3(2):623-637, 2010, doi:10.4271/2010-01-2117.
6. Fushimi, A., Kondo, Y., Kobayashi, S., Fujitani, Y., Saitoh, K., Takami, A., Tanabe, K., "Chemical composition and source of fine and nanoparticles from recent direct injection gasoline passenger cars: Effects of fuel and ambient temperature," J. of Atmospheric Environment, 124. A: 77-84, 2016, doi:10.1016/j.atmosenv.2015.11.017
7. Haynes, B.S. and Wagner, H. G., "Soot Formation," J. of Prog. Energy Combust. Sci., vol. 7, 229-273, 1981, doi:10.1016/0360-1285(81)90001-0
8. Kittelson, D.B., "Engines and nanoparticles: a review," J. of Aerosol Science, 29 (5-6), 575-588, ISSN 0021-8502, doi:10.1016/S0021-8502(97)10037-4.
9. Graskow, B., Kittelson, D., Abdul-Khalek, I., Ahmadi, M. et al., "Characterization of Exhaust Particulate Emissions from a Spark Ignition Engine," SAE Technical Paper 980528, 1998, doi:10.4271/980528.
10. Dec, J., "A Conceptual Model of DI Diesel Combustion Based on Laser-Sheet Imaging," SAE Technical Paper 970873, 1997, doi:10.4271/970873.
11. Glassman, I. and Yetter, RA, "Combustion, Fourth edition," Academic Press, Burlington, 2008.
12. Amanna, C. A. and Sieglaa, D. C., "Diesel Particulates—What They Are and Why," J. of Aerosol Science and Technology, vol.1, 1:73-101, 1981, doi:10.1080/02786828208958580.
13. World health report 2002. Geneva: World Health Organization; 2002, Available from: http://www.who.int/whr/2002/en/whr02_en.pdf?ua=1
14. Brook R, Rajagopalan S, Pope A, Brook J, Bhatnagar A, Diez-Roux A, et al. Particulate matter air pollution and cardiovascular disease: an update to the scientific statement from the American Heart Association. Circulation. 2010;121:2331–2378, doi: 10.1161/CIR.0b013e3181dbece1.
15. Rückerl R, Ibald-Mulli A, Koenig W, Schneider A, Woelke G, et al. Air pollution and markers of inflammation and coagulation in patients with coronary heart disease. Am J Respir Crit Care Med. 2006;173(4):432–441. doi: 10.1164/rccm.200507-1123OC.
16. Hoffmann B, Moebus S, Dragano N, Stang A, Möhlenkamp S, et al. Chronic residential exposure to particulate matter air pollution and systemic inflammatory markers. Environ Health Perspect. 2009;117(8):1302–1308.
17. Sullivan J, Hubbard R, Liu S, Shepherd K, Trenga C, et al. A community study of the effect of particulate matter on blood measures of inflammation and thrombosis in an elderly population. Environ Health. 2007;6:3. doi: 10.1186/1476-069X-6-3.
18. Forbes L, Patel M, Rudnicka A, Cook D, Bush T, et al. Chronic exposure to outdoor air pollution and markers of systemic inflammation. Epidemiology. 2009;20(2):245–253. doi: 10.1097/EDE.0b013e318190ea3f.
19. Pope C, Burnett R, Thurston G, Thun M, Calle E, et al. Cardiovascular mortality and long-term exposure to particulate air pollution. Circulation. 2004;109:71–77. doi: 10.1161/01.CIR.0000108927.80044.7F.
20. Hogg J, Chu F, Utokaparch S, Woods R, Elliott W, et al. The nature of small-airway obstruction in chronic obstructive pulmonary disease. NEJM. 2004;350(26):2645–2653. doi: 10.1056/NEJMoa032158.
21. Behndig A, Mudway I, Brown J, Stenfors N, Helleday R, et al. Airway antioxidant and inflammatory responses to diesel exhaust exposure in healthy humans. Eur Resp J. 2006;27:359–365. doi: 10.1183/09031936.06.00136904.
22. Desqueyroux H, Pujet J, Prosper M, Squinzai F, Momas I. Short-term effects of low-level air pollution on respiratory health of adults suffering from moderate to severe asthma. Environ Res. 2002;89:29–37. doi: 10.1006/enrs.2002.4357.
23. Gent J, Koutrakis P, Belanger B, Triche E, Holford T, et al. Symptoms and medication use in children with asthma and traffic-related sources of fine particle pollution. Environ Health Perspect. 2009;117(7):1168–1174. doi: 10.1289/ehp.0800335
24. Goss C, Newsom S, Scholdcrout J, Sheppard L, Kaufman J. Effect of ambient air pollution on pulmonary exacerbations and lung function in cystic fibrosis. Am J Resp Crit Care Med. 2004;169:816–821. doi: 10.1164/rccm.200306-779OC.
25. Wellenius G, Schwartz J, Mittleman M. Air pollution and hospital admissions for ischemic and hemorrhagic stroke among Medicare beneficiaries. Stroke. 2005;36(12):2549–2553. doi: 10.1161/01.STR.0000189687.78760.47.
26. O'Donnel M, Fang J, Mittleman M, Kapral M, Wellenius G, et al. Fine particulate air pollution (PM2.5) and the risk of acute ischemic stroke. Epidemiology. 2011;22(3):422–431. doi: 10.1097/EDE.0b013e3182126580.
27. Henrotin J, Besancenot J, Bejot Y, Giroud M. Short-term effects of ozone air pollution on ischaemic stroke occurrence: a case-crossover analysis from a 10-year population-based study in Dijon, France. Occup Environ Med. 2007;64(7):439–445, doi: 10.1136/oem.2006.029306.
28. United States Environmental Protection Agency. Particulate Matter. Retrieved on February 12, 2014 from http://cfpub.epa.gov/airnow/index.cfm?action=aqibasics.particle, accessed Nov. 2015
29. Bond, T. C., et al. (2013), Bounding the role of black carbon in the climate system: A scientific assessment, J. Geophys. Res. Atmos., 118, 5380–5552, doi:10.1002/jgrd.50171.

30. EC, 2012. Commission Regulation 459/2012. Available from: http://eur-lex.europa.eu/LexUriServ/LexUriServ.do?uri=OJ:L:2012:142:0016:0024:en:PDF, accessed Jun. 2016
31. Mamakos, A., Dardiotis, C., & Martini, G., (2011). "Assessment of Particle Number Limits for Petrol Vehicles," JRC Report, Available from: http://circa.europa.eu/Public/irc/enterprise/automotive/library?l=/commission_expert/vehicle_emissions/107th_january_2011/20110124_circapdf/_EN_1.0_&a=d0110124_circapdf/_EN_1.0_&a=d.
32. Zhan, R., Eakle, S., and Weber, P., "Simultaneous Reduction of PM, HC, CO and NOx Emissions from a GDI Engine," SAE Technical Paper 2010-01-0365, 2010, doi:10.4271/2010-01-0365.
33. Chan, T., Meloche, E., Kubsh, J., Rosenblatt, D. et al., "Evaluation of a Gasoline Particulate Filter to Reduce Particle Emissions from a Gasoline Direct Injection Vehicle," SAE Int. J. Fuels Lubr. 5(3):1277-1290, 2012, doi:10.4271/2012-01-1727.
34. Reghunathan Nair, A., Schubring, B., Premchand, K., Brocker, A. et al., "Methodology to Determine the Effective Volume of Gasoline Particulate Filter Technology on Criteria Emissions," SAE Technical Paper 2016-01-0936, 2016, doi:10.4271/2016-01-0936.
35. Parks, J., Storey, J., Prikhodko, V., Debusk, M. et al., "Filter-based control of particulate matter from a lean gasoline direct injection engine," SAE Technical Paper 2016-01-0937, 2016, doi:10.4271/2016-01-0937.
36. Saito, C., Nakatani, T., Miyairi, Y., Yuuki, K. et al., "New Particulate Filter Concept to Reduce Particle Number Emissions," SAE Technical Paper 2011-01-0814, 2011, doi:10.4271/2011-01-0814.
37. Ito, Y., Shimoda, T., Aoki, T., Yuuki, K. et al., "Next Generation of Ceramic Wall Flow Gasoline Particulate Filter with Integrated Three Way Catalyst," SAE Technical Paper 2015-01-1073, 2015, doi:10.4271/2015-01-1073.
38. Ogyu, K., Ogasawara, T., Nagatsu, Y., Yamamoto, Y. et al., "Feasibility Study on the Filter Design of Re-Crystallized SiC-GPF for TWC Coating Application," SAE Technical Paper 2015-01-1011, 2015, doi:10.4271/2015-01-1011.
39. Mamakos, A., Steininger, N., Martini, G., Dilara, P., Drossinos, Y., "Cost effectiveness of particulate filter installation on Direct Injection Gasoline vehicles," J. of Atmospheric Environment, 77:16-23, 2013, doi:10.1016/j.atmosenv.2013.04.063
40. Velji A, Yeom K, Wagner U, Spicher U et al. "Investigations of the formation and oxidation of soot inside a direct injection spark ignition engine using advanced laser-techniques". SAE technical paper 2010–01-0352; 2010.
41. Maricq MM, Podsiadlik DH, Brehob DD, Haghgooie M., "Particulate emissions from a direct-injection spark-ignition (DISI) engine". SAE technical Paper 1999–01-1530; 1999.
42. Kayes D, Hochgreb S. "Mechanisms of particulate matter formation in spark ignition engines. 1. Effect of engine operating conditions". Environ Sci Technol 1999;33(22):3957–67.
43. Price P, Stone R, Collier T, Davies M., "Particulate matter and hydrocarbon emissions measurements: comparing first and second generation DISI with PFI in single cylinder optical engines". SAE technical paper 2006–01-1263; 2006.
44. Bonatesta F., Chiappetta E., La Rocca A., "Part-load particulate matter from a GDI engine and the connection with combustion characteristics," Applied Energy 124 (2014) 366–376, doi:10.1016/j.apenergy.2014.03.030.
45. Mamakosa, A., Martinia, G., Marottaa, A., Manfredia, U., "Assessment of different technical options in reducing particle emissions from gasoline direct injection vehicles," J. of Aerosol Science, 63, 115–125, doi: 10.1016/j.jaerosci.2013.05.004.
46. Piock, W., Hoffmann, G., Berndorfer, A., Salemi, P. et al., "Strategies Towards Meeting Future Particulate Matter Emission Requirements in Homogeneous Gasoline Direct Injection Engines," SAE Int. J. Engines 4(1):1455-1468, 2011, doi:10.4271/2011-01-1212.
47. Whitaker, P., Kapus, P., Ogris, M., and Hollerer, P., "Measures to Reduce Particulate Emissions from Gasoline DI engines," SAE Int. J. Engines 4(1):1498-1512, 2011, doi:10.4271/2011-01-1219.
48. McAllister, M., Smith, S., Kapus, P., Vidmar, K. et al., "EU6c Particle Number on a Full Size SUV - Engine Out or GPF," SAE Int. J. Fuels Lubr. 7(3):995-1003, 2014, doi:10.4271/2014-01-2848.
49. Lattimore, T., Wang, C., Xu H., Wyszynski, M. L., Shuaib S., "Investigation of EGR Effect on Combustion and PM Emissions in a DISI Engine," J. Applied Energy 161:256–267, doi:10.1016/j.apenergy.2015.09.080
50. Kazour, J., Befrui, B., Husted, H., Raney, M. et al., "Innovative Sprays and Particulate Reduction with GDi Injectors," SAE Technical Paper 2014-01-1441, 2014, doi:10.4271/2014-01-1441.
51. Hoffmann, G., Befrui, B., Berndorfer, A., Piock, W. F., Varble, D. L., "Influence of GDi multi-hole fuel system pressure on spray and engine emissions," Fuel Systems for IC Engines, IMechE, London, 2015.
52. Anbari Attar, M., Badawy, T., Xu, H., "Effects of injector nozzle deposit on spray pattern and mixture preparation in an optical DISI engine," Fuel Systems for IC Engines: IMechE, London, 2015.
53. Berndorfer A., Breuer S., Piock W.F., Von Bacho P.: "Diffusion Combustion Phenomena in GDi Engines caused by Injection Process," SAE 2013-01-0261.
54. Anbari Attar, M., Badawy, T., Xu, H., "Optical investigation of influence of injector nozzle deposit on particulate matter emissions drift," Internal Combustion Engines, IMechE, London, 2015.
55. Pilch, M., Erdman, C. A., "Use of Breakup Time Data and Velocity History Data to Predict the Maximum Size of Stable Fragments for Acceleration-Induced Breakup of a Liquid Drop," Int. J. Multiphase Flow, 13, 741-757, 1987, doi:10.1016/0301-9322(87)90063-2.
56. Shibata, H., Kito, T., Saitoh, S., Walford, M., Williams, I., Kaneta, H., "Gasoline direct injection spray improvements for future emission legislation," Fuel Systems for IC Engines: IMechE, London, 2015.
57. Hoffmann, G., Befrui, B., Berndorfer, A., Piock, W. et al., "Fuel System Pressure Increase for Enhanced Performance of GDi Multi-Hole Injection Systems," SAE Int. J. Engines 7(1):519-527, 2014, doi:10.4271/2014-01-1209.
58. Symonds, J. P. R., Reavell, K. St. J., Olfert, J. S., Campbell, B. W., Swift, S. J., "Diesel soot mass calculation in real-time with a differential mobility spectrometer", J. of Aerosol Science, 38 (1): 52–68, doi:10.1016/j.jaerosci.2006.10.001.
59. Symonds, J. P. R, "Calibration of Fast Response Differential Mobility Spectrometers", Available from: http://www.npl.co.uk/upload/pdf/20100608_mansa_symonds.pdf
60. Cavina, N., Poggio, L., Bedogni, F., Rossi, V. et al., "Benchmark Comparison of Commercially Available Systems for Particle Number Measurement," SAE Technical Paper 2013-24-0182, 2013, doi:10.4271/2013-24-0182.
61. Lüders H., Krüger M., Stommel P. and Lüers B. (1998). "The Role of Sampling Conditions in Particle Size Distribution Measurements". SAE Technical Paper 981374.
62. Swanson J., Kittelson D. (2010). "Evaluation of thermal denuder and catalytic stripper methods for solid particle measurements". J. of Aerosol Science, 41: 1113-1122, doi:10.1016/j.jaerosci.2010.09.003.

63. Johansson, A., Hemdal, S., Dahlander, P., "Experimental Investigation of Soot in a Spray-Guided Single Cylinder GDI Engine Operating in a Stratified Mode," SAE Technical Paper 2013-24-0052, 2013, doi:10.4271/2013-24-0052.
64. Xu, F. and Stone, R., "The Effects of Hot Air Dilution and an Evaporation Tube (ET) on the Particulate Matter Emissions from a Spray Guided Direct Injection Spark Ignition Engine," SAE Technical Paper 2012-01-0436, 2012, doi:10.4271/2012-01-0436.
65. Schreiber, D., Forss, A., Mohr, M., Dimopoulos, P., "Particle Characterisation of Modern CNG, Gasoline and Diesel Passenger Cars," SAE Technical Paper 2007-24-0123, 2007, doi:10.4271/2007-24-0123.
66. Giechaskiel, B., Arndt, M., Schindler, W., Bergmann, A. et al., "Sampling of Non-Volatile Vehicle Exhaust Particles: A Simplified Guide," SAE Int. J. Engines 5(2):379-399, 2012, doi:10.4271/2012-01-0443.
67. Anbari Attar, M., Herfatmanesh, M., R., Zhao, H., Cairns, A., "Experimental investigation of direct injection charge cooling in optical GDI engine using tracer-based PLIF technique," J. of Experimental Thermal and Fluid Science, V. 59: 96-108, doi:10.1016/j.expthermflusci.2014.07.020.
68. Liu, Q., Cairns, A., Zhao, H., Anbari Attar, M., et al., "The effects of charge homogeneity and repeatability on particulates using the PLIF technique in an optical DISI engine," SAE Int. J. of Engines 7(1): 500-518, 2014, doi:10.4271/2014-01-1207.
69. Smith, O. I., "Fundamentals of soot formation in flames with application to diesel engine particulate emissions," J. of Progress in Energy and Combustion Science, 7.4: 275-291, 1981, doi:10.1016/0360-1285(81)90002-2
70. Amann, C., Stivender, D., Plee, S., and MacDonald, J., "Some Rudiments of Diesel Particulate Emissions," SAE Technical Paper 800251, 1980, doi:10.4271/800251.

Highlights:

- We explored impacts of purposed-designed gasoline direct injection fuel delivery systems on engine-out particulate matter emissions.
- We studied effects of fuel flow rate and spray angle on PM emission for homogeneous and heterogeneous in-cylinder fuel/air mixtures.
- We investigated influence of location and relative timing of fuel impingement on engine-out particulate matter emissions.